# Transient Silenes and Their Dimethyl-$d_6$ Ether Donor Complexes from the Gas-Phase Pyrolysis of Siletanes†,‡

Norbert Auner,*,§ Josef Grobe,*,|| Thomas Müller,§,⊥ and Horst W. Rathmann||

*Institut für Anorganische Chemie der Johann Wolfgang Goethe Universität Frankfurt am Main, Marie-Curie Strasse 11, 60439 Frankfurt, FRG, Fachinstitut für Anorganische Chemie der Humboldt Universität Berlin, Hessische Strasse 1-2, D-10115 Berlin, FRG, and Institut für Anorganische Chemie der Westfälischen Wilhelms-Universität Münster, Wilhelm-Klemm-Strasse 8, D-48149 Münster, FRG*

*Received March 30, 2000*

The silenes $H_2Si{=}CH_2$ (**2**), $MeHSi{=}CH_2$ (**7**), and $Me_2Si{=}CH_2$ (**8**) have been prepared by low-pressure flow pyrolysis from the corresponding siletanes $H_2SiCH_2CH_2CH_2$ (**1**), $MeHSiCH_2CH_2CH_2$ (**5**), and $Me_2SiCH_2CH_2CH_2$ (**6**). **2**, **7**, and **8** were identified by residual gas analysis of the pyrolysis stream and by low-temperature NMR spectroscopy of their complexes **2**·$O(CD_3)_2$ (**16**), **7**·$O(CD_3)_2$ (**17**), and **8**·$O(CD_3)_2$ (**18**). The complexes **16**−**18** are stable to temperatures between −140 and −100 °C. Above these temperatures rapid polymerization occurs. The complexation with dimethyl ether obviously stabilizes the silenes and allows their spectroscopic investigation. The $^{29}Si$ chemical shifts of the complexes are −25.2 (**16**), −1.8 (**17**) and 16.8 ppm (**18**). The experimental results are supported by ab initio and density functional calculations of geometries and magnetic properties of the silenes **2**, **7**, and **8** and the dimethyl ether complexes **16**−**18**. The calculations predict a relatively short Si−O separation of about 1.7 Å in the corresponding silene−ether adducts. Natural bond analysis of the donor−acceptor complex **16** reveals that the interaction between the ether molecule and the silene is predominantly ionic, despite the relatively short Si−O distance.



## Introduction

The gas-phase thermal decomposition of siletanes has been of long-standing interest, since it was historically the first method to produce silenes as reactive intermediates.[1] The landmark paper by Gusel'nikov and Flowers,[2] which demonstrated that 1,1-dimethylsiletane decomposes thermally to 1,1-dimethylsilene and ethene, was the starting point for numerous investigations of the thermal decomposition of siletanes.[1] Mechanistic studies,[3] as well as recent ab initio calculations,[4] suggest that silene formation proceeds via initial homolytic C−C bond cleavage with the formation of a CC-centered biradical, followed by rupture of the central Si−C bond as shown in Scheme 1. According to calculations at the MRMP/6-311G(d,p) level, the biradical is not an intermediate and this reaction might be viewed as a highly asynchronous concerted route to silene and ethene, a route along which there is considerable diradical character.[4a]

This reaction sequence is well-supported for the pyrolysis of 1,1-disubstituted siletanes by chemical trapping experiments,[5] by IR spectroscopy of the matrix-isolated products,[6] and by direct gas-phase measurements on the pyrolysis stream.[7] However, the mechanism of the pyrolysis of siletanes with one or two hydrogens on the silicon still is controversial. Conlin and Gill demonstrated convincingly that during the pyrolysis of siletane **1** silene, silylene, methylsilylene, and propene are formed (Scheme 2).[8]

The formation of methylsilylene can be rationalized by isomerization of silene **2** via a 1,2-hydrogen shift.[9]

* To whom correspondence should be addressed. Fax: N.A., +6979829188; J.G., +2518333108.

† This paper is dedicated to Prof. Robert West, for his outstanding contributions to organosilicon chemistry.

‡ Presented in part on the XIth International Symposium on Organosilicon Chemistry, Montpellier, France, 1996.

§ Johann Wolfgang Goethe Universität Frankfurt am Main.

⊥ Humboldt Universität Berlin.

|| Westfälischen Wilhelms-Universität Münster.

(1) Recent reviews on silenes and related compounds: (a) Raabe, G.; Michl, J. In *The Chemistry of Organic Silicon Compounds*; Rappoport, Z., Patai, S., Eds.; Wiley: New York, 1989; Vol. 1, p 1015. (b) Brook, A. G.; Brook, M. A. *Adv. Organomet. Chem.* **1995**, *39*, 125. (c) Müller, T.; Ziche, W.; Auner, N. In *The Chemistry of Organic Silicon Compounds*; Rappoport, Z., Apeloig, Y., Eds.; Wiley: New York, 1998; Vol. 2, p 857.

(2) Gusel'nikov, L. E.; Flowers, M. C. *J. Chem. Soc., Chem. Commun.* **1967**, 864.

(3) (a) Barton, T. J.; Marquardt, G.; Kilgour, J. A. *J. Organomet. Chem.* **1975**, *85*, 317. (b) Golino, C. M.; Bush, R. D.; On, P.; Sommer, L. H. *J. Am. Chem. Soc.* **1975**, *39*, 3543. (c) Gusel'nikov, L. E.; Nametkin, N. S.; Dolgopolov, N. N. *J. Organomet. Chem.* **1979**, *169*, 165.

(4) (a) Gordon, M. S.; Barton, T. J.; Nakano, H. *J. Am. Chem. Soc.* **1997**, *119*, 1966. (b) Skanke, P. N.; Schaad, L. J. *J. Phys. Chem. A* **1997**, *101*, 7408.

(5) For examples see: Raabe, G.; Michl, J. *Chem. Rev.* **1985**, *85*, 419 and references therein.

(6) For example see: (a) Gusel'nikov, L. E.; Volkova, V. V.; Avakyan, V. G.; Nametkin, N. S. *J. Organomet. Chem.* **1980**, *201*, 137. (b) Nefedov, O. M.; Maltsev, A. K.; Khabashesku, V. N.; Korolev, V. A. *J. Organomet. Chem.* **1980**, *201*, 123.

(7) (a) Auner, N.; Grobe, J. *Z. Anorg. Allg. Chem.* **1979**, *459*, 15. (b) Basu, S.; Davidson, I. M. T.; Laupert, R.; Potzinger, P. *Ber. Bunsen-Ges. Phys. Chem.* **1979**, *83*, 1282. (c) Koenig, T.; McKenna, W. J. *J. Am. Chem. Soc.* **1981**, *103*, 1212. (d) Dyke, J. M.; Josland, G. D.; Lewis, R. A.; Morris, A. *J. Phys. Chem.* **1982**, *86*, 2913.

(8) Conlin, R. T.; Gill, R. S. *J. Am. Chem. Soc.* **1983**, *105*, 618.

10.1021/om0002778 CCC: $19.00 
Publication on Web 07/29/2000

**Scheme 1**

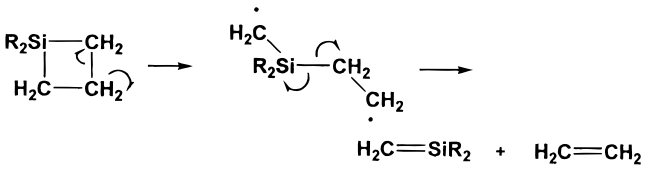

**Scheme 2**

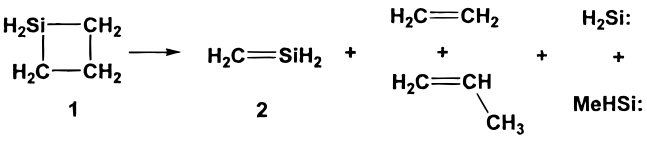

**Scheme 3**

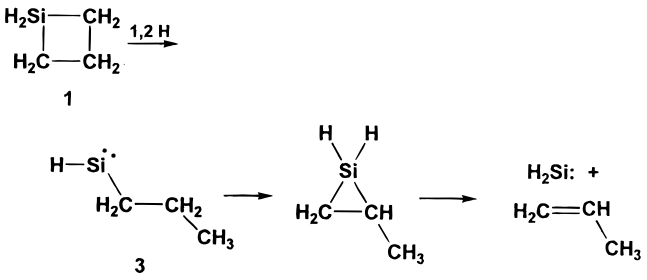

The formation of propene, however, was explained by an alternative mechanism involving concerted ring opening and 1,2-H shift to form propylsilylene **3** (Scheme 3).[10] In agreement with this reaction pathway recent ab initio calculations predict the production of **3** to be thermodynamically and kinetically competitive with the formation of silene.[4a]

Despite considerable experimental efforts,[11] no direct spectroscopic evidence for the formation of **2** during the pyrolysis of **1** could be obtained until very recently. Bailleux et al. obtained a millimeter microwave spectrum of **2** produced by thermal decomposition of **1**.[12] 5,6-Bis(trifluoromethyl)-2-silabicyclo[2.2.2]octa-5,7-diene (**4**) proved to be a more useful precursor for high-yield production of silene **2**,[13] and the microwave data obtained were identical with those from the thermal decomposition of siletane **1** (Scheme 4).[12a]

We report here our study of the low-pressure flow pyrolysis of siletanes **1**, **5**, and **6** and the identification of silenes **2**, **7**, and **8** by mass spectrometry and low-temperature NMR spectroscopy (Scheme 5).

**Scheme 4**

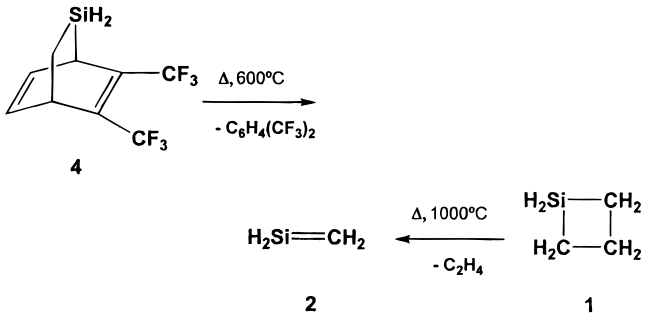

**Scheme 5**

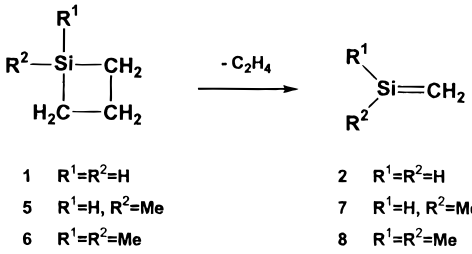

**Experimental Results**

The low-pressure pyrolysis experiments were performed in a special pyrolysis apparatus coupled to an NMR cooling trap, which is described in detail in the Supporting Information.[14] The final vacuum in the complete pyrolysis system could be adjusted to $(1.5-2) \times 10^{-9}$ mbar, and when the pyrolysis experiments are performed, the pressure rises typically to $10^{-4}-10^{-5}$ mbar. These UHV conditions are essential, because the particle density decreases within the pyrolysis tube and the cooling trap to approximately $3 \times 10^7$ cm$^{-3}$ ($10^{-9}$ mbar) and $5 \times 10^{11}$ cm$^{-3}$ ($10^{-5}$ mbar). These particle densities are equivalent to mean free path lengths of $6.9 \times 10^4$ and 6 m, respectively.[15] Under these UHV conditions the possibility for reactive particle interactions is minimized during the pyrolysis and the pyrolytically generated molecules can be collected in the cooling trap without collisions with other molecules. The chemical composition of the pyrolysis gas stream was continuously analyzed by a quadrupole mass spectrometer, and thus the optimal pyrolysis conditions with respect to thermolysis temperature and pressure could be determined in previous runs.[16] This is shown, for example, for the decomposition of **1** in Figure 1.

Up to an oven temperature of 560 °C the MS spectra of the pyrolysis gas show exclusively the fragmentation pattern of **1** (Figure 1a). At temperatures higher than 800 °C mass peaks at *m*/*z* 44 and 28, typical for silene **2** and ethene, respectively, become more abundant at

(9) (a) Goddard, J. D.; Yoshioka, Y.; Schaefer, H. F., III. *J. Am. Chem. Soc.* **1980**, *102*, 7644. (b) Nagase, S.; Kudo, T. *J. Chem. Soc. Chem. Commun.* **1983**, 141. (c) Drahnak, T. J.; Michl, J.; West, R. *J. Am. Chem. Soc.* **1981**, *103*, 1845. (d) Conlin, R. T.; Wood, D. L. *J. Am. Chem. Soc.* **1981**, *103*, 1843. (e) Arrington, C. A.; West, R.; Michl, J. *J. Am. Chem. Soc.* **1983**, *105*, 6176. (f) Barton, T. J.; Burns, S. A.; Burns, G. T. *Organometallics* **1982**, *1*, 210. (g) Walsh, R. *J. Chem. Soc., Chem. Commun.* **1982**, 1415.

(10) Davidson, I. M. T.; Fenton, A.; Ijadi-Maghsoodi, S.; Scampton, R. J.; Auner, N.; Grobe, J.; Tillman, N.; Barton, T. J. *Organometallics* **1984**, *3*, 1593.

(11) Auner, N.; Grobe, J. Unpublished results. For attempts to characterize the silenes **2**, **7**, and **8** by mass spectroscopy, see ref 7a.

(12) (a) Bailleux, S.; Bogey, M.; Breidung, J.; Bürger, H.; Fagjar, R.; Liu, Y.; Pola, J.; Senzlober, M.; Thiel, W. *Angew. Chem., Int. Ed. Engl.* **1996**, *35*, 2513. (b) Bailleux, S.; Bogey, M.; Demaison, J.; Bürger, H.; Senzlober, M.; Liu, Y.; Breidung, J.; Thiel, W.; Fagjar, R.; Pola, J. *J. Chem. Phys.* **1997**, *106*, 10016.

(13) (a) Mihm, G.; Reisenauer, H. P.; Maier, G. *Angew. Chem., Int. Ed. Engl.* **1981**, *20*, 597. (b) Bock, H.; Solouki, B.; Maier, G.; Mihm, G.; Rosmus, P. *Angew. Chem., Int. Ed. Engl.* **1981**, *20*, 598. (c) Mihm, G, Reisenauer, H. P.; Maier, G. *Chem. Ber.* **1984**, *117*, 2351.

(14) Rathmann, H. W. Ph.D. Thesis, Münster, Germany, 1985.

(15) Calculations used the hard sphere model approximation in the kinetic theory of gases. The mean free path $l$ is related to the collision diameter $d$ by $l = kT/(\pi 2^{1/2} p d^2)$, where $p$ is the pressure, $T$ the absolute temperature, and $k$ the Boltzmann constant. For $d$ the value of air was used: $d = 3.66 \times 10^{-10}$ m. From: *CRC Handbook of Chemistry and Physics*, 79th ed.; Lide, D. R., Ed.; CRC Press: Boca Raton, FL, 1998; pp 6−44.

(16) Copyrolysis experiments with 2,3-dimethyl-1,3-butadiene at $10^{-2}$ mbar gave for **5** and **6** product distributions, namely 1,3-disilacyclobutanes and 1-silacyclo-3-hexenes, similar to those found by others under comparable conditions.[9d,f,17] Similar experiments with **1** were unsuccessful; only polymeric material accompanied by methylsilane, propene, and ethene was detected.

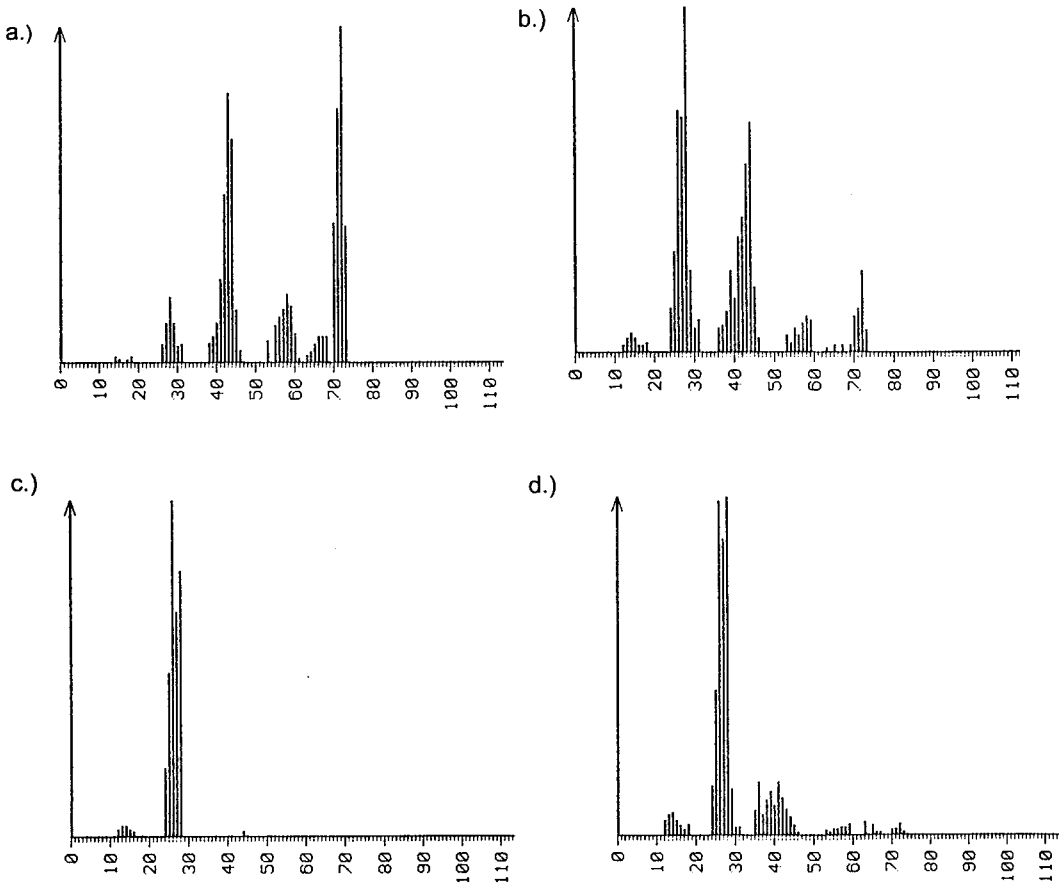


**Figure 1.** Mass spectra of the pyrolysis gas stream of **1** at several oven temperatures: (a) at 560 °C; (b) at 920 °C; (c) at 920 °C with cooling trap at −196 °C; (d) at 1100 °C.



the expense of mass peaks characteristic for **1** (Figure 1b). Further increase of temperature leads to a decrease of the intensity of the mass peak *m*/*z* 44 relative to that at *m*/*z* 28, indicating the beginning decomposition of **2** at oven temperatures of 1100 °C (Figure 1d). The optimum ratio between **2** and **1** of 2.8:1 is obtained at temperatures around 900 °C. When the pyrolysis stream was passed through a liquid nitrogen cooling trap, the peaks resulting from ionization of ethene dominated the mass spectra (Figure 1c). Thus, even at this temperature ethene could not be condensed under the applied low-pressure pyrolysis conditions. The small residual peak at *m*/*z* 44 indicates that only minor amounts of silene **2** could escape from the cooling trap.

Generally, in a typical run 10 mmol of the siletane was thermolyzed over a period of 6 days at 900−1000 °C. The pyrolysis products were collected and condensed in the cooling trap at −196 °C, while most of the ethene produced was pumped off, even at this low temperature. The molten glasslike, highly viscous condensate then was transferred into an adjoining 10 mm NMR tube. As lock compound and solvent for the NMR measurements, 2.5 mL of dimethyl ether-$d_6$ and dichlorodifluoromethane in an approximately 1:4 ratio was condensed into the NMR tube after the pyrolysis was completed. This mixture remains liquid even at about −140 °C, the temperature required for the NMR measurements. Residual ethene was pumped off at −196 °C, and then the NMR tube was sealed under ultrahigh vacuum (approximately $10^{-9}$ mbar) and was stored in liquid nitrogen until the NMR investigations were performed.

**Pyrolysis of Siletane 1.** Several pyrolysis experiments with **1** at 1000 °C over 6 days gave a highly viscous, glasslike liquid. Upon addition of the $(D_3C)_2O/CF_2Cl_2$ mixture clear solutions of **2** were obtained which showed in the $^{29}$Si NMR spectrum, recorded at −140 °C, a triplet at −25.2 ppm ($^1J_{SiH}$ = 193 Hz) indicating the presence of an $SiH_2$ group. No other silicon-containing compound could be detected; in particular, no residual signal due to siletane **1** could be observed.[18] Obviously, the concentration of **1** in the resulting solution was negligibly small. The intensity of the triplet at −25.2 ppm was found to be extremely temperature sensitive. Thus, warming the NMR sample to −100 °C caused rapid decomposition of the observed highly reactive species, as indicated by the dramatically decreasing peak intensity (see Figure 2).

Interestingly, formation of other silicon-containing compounds could not be detected. Even no 1,3-disiletane[19] was formed, characterized by others as the subsequent product of silene dimerization in the gas phase or of the annealing of an argon matrix to 35 K.[13] This finding suggests a rapid polymerization of silene **2** in the condensed phase even at −100 °C. From this a white, polymeric, waxy solid was isolated at room

(17) (a) Nametkin, N. S.; Vdovin, V. M.; Gusel'nikov, L. E.; Zavylov, V. I. *Izv. Akad. Nauk SSSR, Ser. Khim.* **1966**, 586. (b) Nametkin, N. S.; Gusel'nikov, L. E.; Vdovin, V. M.; Grinberg, P. L.; Zavylov, V. I.; Oppengeim, V. D. *Dokl. Akad. Nauk SSSR* **1966**, *171*, 630. (c) Gusel'nikov, L. E.; Nametkin, N. S. *Chem. Rev.* **1979**, *79*, 529. (d) Maltsev, A. K.; Khabashesku, V. N.; Nefedov, O. M. *Dokl. Akad. Nauk SSSR* **1979**, *247*, 283.

(18) **1**: $\delta(^{13}C)$ 10.8 ($C_\alpha$), 22.8 ($C_\beta$); $\delta(^{29}Si)$ −24.7 ($^1J_{SiH}$ = 190 Hz). **5**: $\delta(^{29}Si)$ −0.6 ($^1J_{SiH}$ = 186 Hz). **6**: $\delta(^{29}Si)$ 18.1.

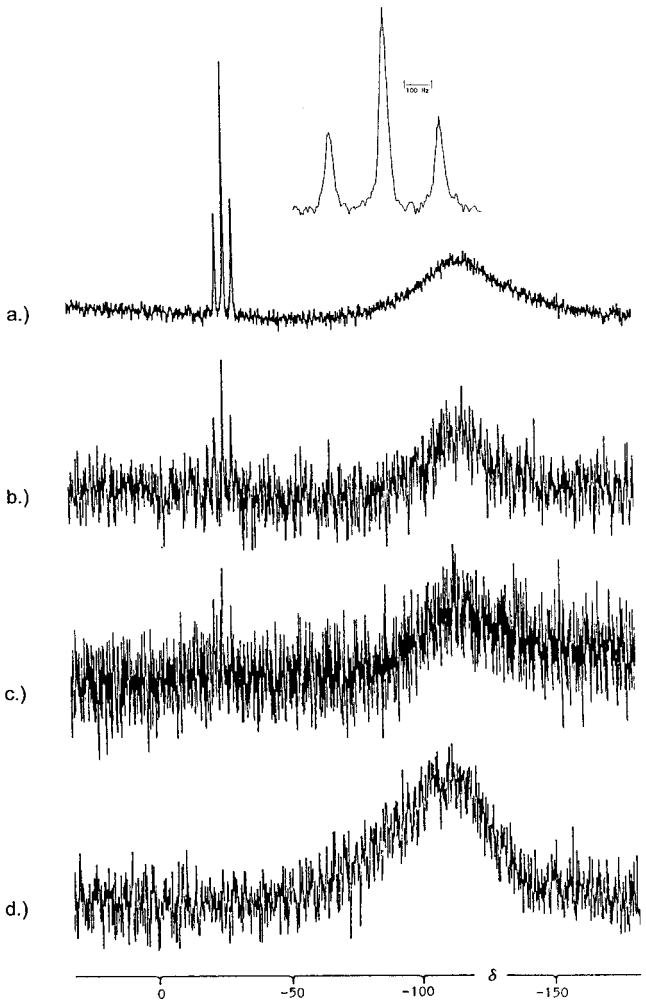


**Figure 2.** 59.6 MHz $^{29}$Si NMR spectra of the pyrolysis product resulting from **1** in $CF_2Cl_2/(D_3C)_2O$ at several temperatures: (a) at −140 °C; (b) at −100 °C, after 2 min; (c) at −100 °C, after 8 min; (d) at −80 °C, after 10 min.

temperature. A field-ionization MS analysis of the crude product confirmed its composition as $(H_2SiCH_2)_n$, indicating the occurrence of longer carbosilane chains.[20,21] At −140 °C the proton-coupled $^{13}$C NMR spectrum ofthe solution consists of four multiplets in addition to the signals of the solvent $CF_2Cl_2$ ($\delta(^{13}C)$ 127.3, $^1J_{CF}$ = 324 Hz)[22a] and dimethyl ether-$d_6$ ($\delta(^{13}C)$ 59.4 $^1J_{CD}$ = 21.0 Hz)[22b] (see Figure 3). A doublet at 133.7 ppm ($^1J_{CH}$ = 158 Hz), a triplet at 116.1 ppm ($^1J_{CH}$ = 154 Hz), and the quartet at 21.5 ppm ($^1J_{CH}$ = 128 Hz) clearly characterized propene,[22c] which is formed during the pyrolysis of **1** according to the reaction sequence shown in Scheme 3.[10,13a,c,17d]

The remaining triplet at $\delta$ 10.8 ($^1J_{CH}$ = 137 Hz) indicates the presence of a $CH_2$ group as part of the pyrolytically generated molecule. The four multiplets show the same temperature dependence as the triplet in the $^{29}$Si NMR spectrum. The signals characterizing propene disappear, probably because propene becomes involved in the polymerization process of the reactive species.

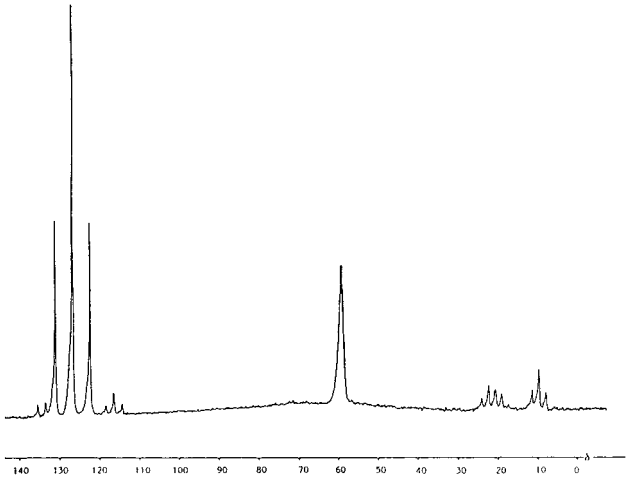


**Figure 3.** 75.5 MHz $^{13}$C NMR spectrum of the pyrolysis product resulting from **1** in $CF_2Cl_2/(D_3C)_2O$ at −140 °C.

The $^1$H NMR showed only a complex, broad multiplet at $\delta$ 5.80−6.90, which exhibits a temperature dependence similar to that for the signals in the $^{29}$Si and $^{13}$C NMR spectra.

In conclusion, the $^1$H, $^{13}$C, and $^{29}$Si NMR experimental results indicate the formation of a highly reactive species composed of a $SiH_2$ and a $CH_2$ group.

At first glance, there is some controversy concerning silene **2**. Formed by gas-phase pyrolysis of **4**, it dimerizes to 1,3-disilacyclobutane on annealing a noble gas matrix from 10 to 35 K. Obviously, the course of the pyrolysis and the silene formation is strongly dependent on the reaction conditions. Maier and co-workers formed, isolated, and characterized silene **2** in high dilution in an argon matrix. Slow annealing as the temperature was increased may have caused a controlled diffusion to yield the 1,3-disilacyclobutane, while in the present case silene **2** was frozen as a pure compound to a glasslike solid with high particle density. Thus, increasing the temperature causes immediate, spontaneous polymerization to give the white, waxy, solid polymer $(H_2SiCH_2)_n$. This is supported by carrying out the pyrolysis experiments using silene precursor **4** under comparable conditions. Silene **2** was formed at temperatures higher than 1173 K (under the conditions published in ref 13, about 670 K is reported to be the optimized pyrolysis temperature) and characterized in the gas phase by mass spectroscopy. 1,2-Bis(trifluoromethyl)benzene was formed as a side product, which severely hinders the transport of the pyrolysis products into the NMR tube because of its comparatively high melting point. Thus, in the course of the sample preparation silene **2** polymerized to a white solid and the formation of 1,3-disilacyclobutane could not be detected. The $^1$H and $^{13}$C NMR spectra of the sample showed signals over the whole spectral range. The most intense occur in the aromatic regions. Obviously, the high pyrolysis temperature required caused an uncontrolled destruction of the silene precursor.[14] The high

(19) See the following examples. $[H_2SiCH_2]_2$: $\delta(^{13}C)$ 7.9; $\delta(^{29}Si)$ 8.3. $[Me_2SiCH_2]_2$: $\delta(^{13}C)$ −3.7; $\delta(^{29}Si)$ −22.1. Fritz, G.; Matern, E. *Z. Anorg. Allg. Chem.* **1976**, *426*, 28.

(20) Similar polymer formation has been reported in the very low pressure pyrolysis of **8**: Nametkin, N. S.; Gusel'nikov, L.; Volvina, E. A.; Vdovin, V. M. *Dokl. Akad. Nauk SSSR* **1975**, *220*, 386.

(21) Polysilaethylene synthesized by the method of Interrante et al. is formed as a yellow liquid, probably due to the lower molecular weight: (a) Shen, Q. H.; Interrante, L. V. *Macromolecules* **1996**, *29*, 5788. (b) Wu, H.-J.; Interrante, L. V. *Macromolecules* **1992**, *25*, 1840.

(22) (a) $\delta(^{13}C)$ 126.2, $^1J_{CF}$ = 325 Hz. (b) $\delta(^{13}C)$ 59.4. (c) $\delta(^{13}C)$ 133.4 ($^1J_{CH}$ = 151.9 Hz), 115.9 ($^1J_{CH}$ = 153.5 Hz, 157.0 Hz), 19.4 ($^1J_{CH}$ = 125.6 Hz). All data are from: Kalinowski, H.-O.; Berger, S.; Braun, S. *$^{13}$C NMR Spectroscopy*; Thieme Verlag: Stuttgart, New York, 1984.

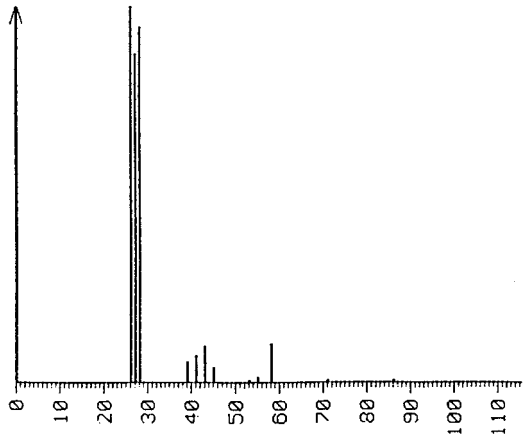


**Figure 4.** Mass spectrum of the pyrolysis gas stream of **5** at 1020 °C.

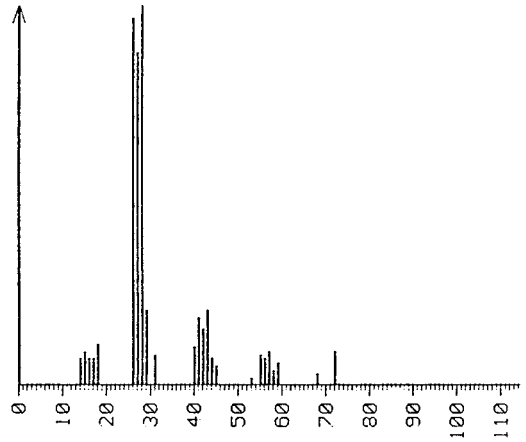


**Figure 5.** Mass spectrum of the pyrolysis gas stream of **6** at 1020 °C.



sensitivity of silene formation to the reaction conditions is further supported by the work of Maltsev et al.,[17d] who, in accordance with Maier's work,[13] could not synthesize **1** from precursor **2**, while Bailleux et al.[12] succeeded in the formation of **1**, performing the gas-phase pyrolysis of **2**, **4**, and even 1,3-disilacyclobutane.

**Pyrolysis of Methylsiletane 5 and of Dimethylsiletane 6.** Low-pressure pyrolysis of **5** and of **6** in separate experiments at 1000 °C gave clear solutions of the pyrolysis products in $(D_3C)_2O/CF_2Cl_2$ (1:4), which were studied by low-temperature $^{29}Si$ NMR spectroscopy. As discussed in detail for siletane **1**, the mass spectroscopic analysis of the pyrolysis gas streams at 1000 °C confirmed the complete degradation of the siletane and the clear formation of the silenes **7** and **8**, respectively, and ethene, characterized by dominant mass peaks in the recorded spectra at *m*/*z* 58, 72, and 28, respectively (see Figures 4 and 5).

The $^{29}Si$ NMR spectrum of the pyrolysis product of **5** at −140 °C showed a single doublet at −1.8 ppm with the coupling constant $^1J_{SiH} = 180$ Hz (Figure 6a). The doublet structure of the signal proves the existence of the SiH group. The detected species decomposes slowly already at −140 °C, and again, as reported for silene **2**, no new silicon-containing compound could be detected. In particular, an indication for either the formation of a dimethylsilylene[23] resulting from a 1,2-hydrogen shift in **7** or the formal [2 + 2] cyclodimerization resulting

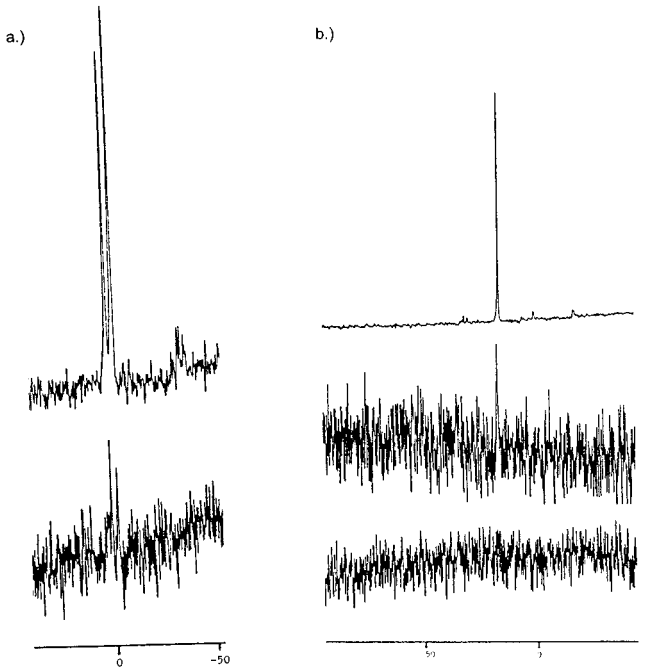


**Figure 6.** 59.6 MHz $^{29}Si$ NMR spectra of the pyrolysis product resulting from (a) **5** in $CF_2Cl_2/(D_3C)_2O$ at −140 °C and (b) **6** in $CF_2Cl_2/(D_3C)_2O$ at −130 °C.

in the corresponding 1,3-disiletane $[Me(H)SiCH_2]_2$[19] could not be observed.

The silene resulting from the pyrolysis of 1,1-dimethylsiletane (**6**) is somewhat more stable than the pyrolysis products of **1** and **5**, as indicated by its temperature-dependent $^{29}Si$ NMR spectra. Decomposition of the generated compound started smoothly after prolonged standing at −100 °C or more rapidly after 10 min at −80 °C, as indicated by the decreasing intensity of the $^{29}Si$ NMR resonance at 16.8 ppm (see Figure 6b).

While the mass spectroscopic analysis of the pyrolysis streams of **1**, **5**, and **6** suggest a clean formation of the respective silenes **2**, **7**, and **8**, the results of the low-temperature NMR investigations cannot be easily interpreted. While the multiplicity of the signals is in convincing agreement with the formation of the simple silenes, the positions of the chemical shifts $\delta(^{29}Si)$ and $\delta(^{13}C)$ are unusual and not in accordance with the presence of triply coordinated silicon and carbon as required for silenes. On the other hand, all literature information about NMR investigations of silenes, especially by $\delta(^{29}Si)$ and $\delta(^{13}C)$[1b,c] spectroscopy, came from silenes, which had bulky substituents on silicon and/or carbon. Nothing is known about the NMR parameters of silenes that contain small substituents. Furthermore, $\delta(^{29}Si)$ and $\delta(^{13}C)$ chemical shifts of the Si=C moiety vary considerably with its substituent pattern. Thus, $\delta(^{29}Si)$ varies from 34.3 ppm for the 2-siloxysilene $(Me_3Si)_2Si{=}C(OSiEt_3)Mes$ (**9**)[24] to 144.2 ppm for the silene

(23) This does not prove the absence of dimethylsilylene since, according to ab initio calculations, dimethylsilylene has a very deshielded silicon atom, resonating at $\delta(^{29}Si)$ 794.4 (GIAO/B3LYP/6-311+G(2df,p)//B3LYP/6-311+G(2df,p)), far beyond the actually observed shift range. For the same reason it would not be possible to detect methylsilylene from the rearrangement of **2**, since calculations predict $\delta(^{29}Si)$ 833.5 (GIAO/B3LYP/6-311+G(2df,p)//B3LYP/6-311+G(2df,p)) (a) Maier, G.; Reisenauer, H. P.; Mihm, G. *Angew. Chem., Int. Ed. Engl.* **1982**, *21*, 854. (b) Maier, G.; Reisenauer, H. P.; Mihm, G. *Chem. Ber.* **1984**, *117*, 2369. (c) Drahnak, T. J.; Michl, J.; West, R. *J. Am. Chem. Soc.* **1981**, *103*, 1845.

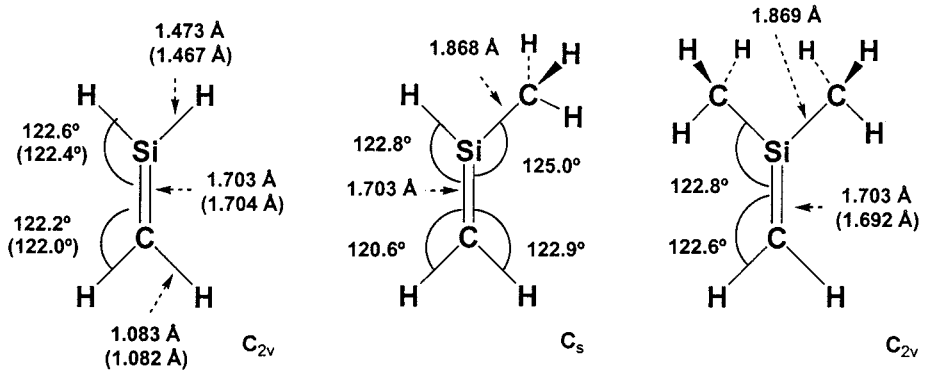


**Figure 7.** Calculated structures of silenes **2**, **7**, and **8** at the B3LYP/6-311+G(2df,p) level. Experimental data from microwave studies are given in parentheses.[12,27]

$Me_2Si{=}C(SiMe_3)SiMe(t\text{-}Bu)_2$ (**10**).[25] The $^{13}C$ chemical shift data cover an even wider range: while the doubly bonded carbon in the siloxysilene $(Me_3Si)_2Si{=}C(OSiMe_3)$-$^1Ad$ (**11**;[26] $^1Ad$ = 1-adamantyl) resonates at 214.2 ppm, this signal appears at only 77.2 ppm in the $^{13}C$ NMR spectrum of **10**.[25] To obtain reliable information about NMR chemical shifts of small silenes such as **2**, **7**, and **8** and their complexes with dimethyl ether, quantum-mechanical calculations of the geometries and magnetic properties were performed.

**Theoretical Results. Silenes.** The calculated structures of the silenes **2**, **7**, and **8** at the B3LYP/6-311+G(2df,p) level are shown in Figure 7. The close resemblance of the calculated geometries of **2** and **8** with recent microwave data[12,27] (Figure 7; experimental data given in parentheses) justifies the use of this computational level of the calculations performed. The silenes **2**, **7**, and **8** are predicted to be planar with identical Si=C bond lengths of 1.703 Å, obviously indicating a negligible substituent effect of a small alkyl group on the Si=C bond length.[28]

Calculated chemical shifts for silenes **2**, **7**, and **8** using the very efficient hybrid density functional GIAO/B3LYP method[29] are summarized in Table 1. For **2** the chemical shifts $\delta(^{29}Si)$ 69.5 and $\delta(^{13}C)$ 115.3 were obtained (Table 1, entry 1). Methyl substitution at silicon in **7** and **8** appears to have a marked influence on the chemical shifts of both doubly bonded atoms. Thus, the silicon in **7** and **8** is even more deshielded than in **2** ($\delta(^{29}Si)$ 104.5 and 133.7, in **7** and **8**, respectively), while the carbon becomes more shielded upon methyl substitution at silicon ($\delta(^{13}C)$ 99.3 and 84.4 in **7** and **8**, respectively).

**Table 1. Calculated and Experimental $\delta(^{29}Si)$ and $\delta(^{13}C)$ Values of Silenes[a]**

| entry | compd | $\delta(^{29}Si)^b$ | $\delta(^{13}C)^b$ |
|---|---|---|---|
| | Calculated Values | | |
| 1 | $H_2Si{=}CH_2$ (**2**) | 69.5 | 115.5 |
| 2 | $H_2Si{=}CH_2$[c] (**2**) | 53.8 | 105.3 |
| 3 | $MeHSi{=}CH_2$ (**7**) | 104.5 | 99.3 |
| 4 | $Me_2Si{=}CH_2$ (**8**) | 133.7 | 84.4 |
| 5 | $Me_2Si{=}C(SiH_3)_2$ (**12**) | 153.9 | 77.2 |
| 6 | $(H_3Si)_2Si{=}CMe_2$ (**13**) | 57.2 | 201.9 |
| | Experimental Values | | |
| 7 | $Me_2Si{=}C(SiMe_3)(SiMe\text{-}t\text{-}Bu_2)$ (**10**) | 144.2 | 77.2 |
| 8 | $(Me_3Si)(t\text{-}BuMe_2Si)Si{=}{}^2Ad$ (**14**)[d] | 51.7 | 196.8 |

[a] B3LYP/6-311+G(2df,p) optimized geometries were used. [b] Relative chemical shifts versus calculated TMS (GIAO/B3LYP/6-311+G(2df,p)//B3LYP/6-311+G(2df,p): $\delta(^{29}Si)$ 328.5, $\delta(^{13}C)$ 183.4). [c] At GIAO/MP2/tz2p(Si,C)dzp(H)//B3LYP/6-311+G(2df,p). Relative chemical shifts versus calculated TMS (GIAO/MP2/tz2p(Si,C)dzp(H)//B3LYP/6-31G(d): $\delta(^{29}Si)$ 371.1, $\delta(^{13}C)$ 198.8). [d] $^2Ad$ = adamantylidene.

The theoretically more reliable GIAO/MP2 method[31] (Table 1, entry 2) for chemical shift calculations predicts for **2** both the silicon and the carbon to be more shielded by 15.7 and 10.2 ppm, respectively. The comparison with the GIAO/B3LYP calculations indicates the known tendency of the density functional based method to overestimate the paramagnetic contributions to the chemical shielding tensor, giving in critical cases overly deshielded chemical shifts.[32] The paramagnetic contribution results from the relatively small HOMO−LUMO gap in the unsaturated silene. However, the fairly good agreement between the computed chemical shifts for the



(24) Ohshita, J.; Masaoka, S.; Hasebe, H.; Ishikawa, M.; Tachinaba, A.; Yano, T.; Yamabe, T. *Organometallics* **1996**, *15*, 3136.
(25) (a) Wiberg, N.; Wagner, G.; Müller, G. *Angew. Chem.* **1985**, *97*, 220; *Angew. Chem., Int. Ed. Engl.* **1985**, *24*, 229. (b) Wiberg, N.; Wagner, G.; Riede, J.; Müller, G. *Organometallics* **1987**, *6*, 32. (c) Wiberg, N.; Wagner, G. *Chem. Ber.* **1986**, *119*, 1467.
(26) (a) Brook, A. G.; Nyburg, S. C.; Abdesaken, F.; Gutekunst, B.; Gutekunst, G.; Kallury, R. K. M. R.; Poon, Y. C.; Chang, Y.-M.; Wong-Ng, W. *J. Am. Chem. Soc.* **1982**, *104*, 5667. (b) Brook, A. G.; Abdesaken, F.; Gutekunst, G.; Plavac, N. *Organometallics* **1982**, *1*, 987.
(27) (a) Chen, J.; Hajduk, P. J.; Keen, J. D.; Chuang, C.; Emilsson, T.; Gutowsky, H. S. *J. Am. Chem. Soc.* **1991**, *113*, 4747. (b) Chen, J.; Hajduk, P. J.; Keen, J. D.; Emilsson, T.; Gutowsky, H. S. *J. Am. Chem. Soc.* **1989**, *111*, 1901.
(28) Apeloig, Y.; Karni, M. *J. Am. Chem. Soc.* **1984**, *106*, 6676.
(29) (a) Ditchfield, R. *Mol. Phys.* **1974**, *27*, 789. (b) Wolinski, K.; Hilton, J. F.; Pulay, P. *J. Am. Chem. Soc.* **1982**, *104*, 5667. (c) Cheeseman, J. R.; Trucks, G. W.; Keith, T. A.; Frisch, M. J. *J. Chem. Phys.* **1996**, *104*, 5497. (d) The SOS/IGLO/DFPT[30] method using basis III predicts similar chemical shifts for **2**: $\delta(^{29}Si)$ 62.9 and $\delta(^{13}C)$ 114.1.
(30) (a) Malkin, V. G.; Malkina, O. L.; Casida, M. E.; Salahub, D. R. *J. Am. Chem. Soc.* **1994**, *116*, 5898. (b) Malkin, V. G.; Malkina, O. L.; Erikson, L. A.; Salahub, D. R. In *Modern Density Functional Theory*; Seminario, J. M., Politzer, P., Eds.; Elsevier: Amsterdam, 1995; p 273. (c) Malkin, V. G.; Malkina, O. L.; Salahub, D. R. *Chem. Phys. Lett.* **1996**, *261*, 335.
(31) (a) Gauss, J. *Chem. Phys.* **1993**, *99*, 3629. (b) For the GIAO/MP2 calculation ACESII was used: Stanton, J. F.; Gauss, J.; Watts, J. D.; Noojien, M.; Oliphant, N.; Perera, S. A.; Szalay, P. G.; Lauderdale, W. J.; Gwaltney, S. R.; Beck, S.; Balkova, A.; Bernholt, D. E.; Baeck, K.-K.; Rozyczko, P.; Sekino, H.; Huber, C.; Bartlett, R. J. ACESII; Quantum Theory Project, University of Florida, Gainesville, FL.
(32) (a) Ottoson, C.-H.; Cremer, D. *Organometallics* **1996**, *15*, 5495. (b) Müller, T.; Zhao, Y.; Lambert, J. B. *Organometallics* **1998**, *17*, 278. (c) For a short review see: Webb, G. A. In *Encyclopedia of Nuclear Magnetic Resonance Spectroscopy*; Grant, D., Webb, G. A., Eds.; Wiley: New York, 1996; p 4316.

**Table 2. Calculated $^1J_{XY}$ Coupling Constants (Hz) in Silenes 2, 7, and 8[a]**

| compd | $^1J_{SiH}$ | $^1J_{CH}$ | $^1J_{Si=C}$ |
|---|---|---|---|
| $H_2Si{=}CH_2$ (**2**) | −231.3 | 149.9 | −104.9 |
| $MeHSi{=}CH_2$ (**7**) | −217.7 | 148.5 | −107.6 |
| $Me_2Si{=}CH_2$ (**8**) | | 146.8 | −108.2 |

[a] Calulated with the SOS DFPT/IGLO method[30] utilizing the Perdew−Wang exchange with Perdew correlation functional[35a,b] and the basis set III[35d] at geometries optimized at the B3LYP/6-311+G(2df,p) level.

model silenes **12** and **13** (Table 1, entries 5 and 6) with the experimental data for the stable silenes **10**[25] and **14**[33] (Table 1, entries 7 and 8) indicates that the chosen theoretical GIAO/B3LYP/6-311+G(2df,p) level is sufficiently accurate, although especially $\delta(^{29}Si)$ is predicted to be too deshielded by approximately 6−10 ppm.

Calculations of the spin−spin coupling constants (see Table 2) using the SOS/DFPT/IGLO method[30b] predict $^1J_{SiH}$ couplings of −231.4 and −217.7 Hz for **2** and **7**, respectively, which are significantly larger than those found for alkylsilanes (e.g., $^1J_{SiH} = -188.6$ and −184.0 Hz for $Me_2SiH_2$ and $Me_3SiH$,[34a] respectively). The calculated $^1J_{CH}$ coupling constants for the triply coordinated carbon atoms in **2**, **7**, and **8** are, however, comparatively smaller than $^1J_{CH}$ couplings found in alkenes.[22c] Coupling constants across the Si=C double bonds are known for several 2-siloxysilenes[34b] and can, therefore, be used to test the reliability of the used theoretical approach. For the model 2-siloxysilene $(H_3Si)_2Si{=}C(OSiH_3)CH_3$, $^1J_{Si=C} = -90.6$ Hz is predicted[34c] to be very near to the experimental data for the 2-siloxysilene **11** ($|^1J_{Si=C}| = 84.4$ Hz).[34b] The computed $^1J_{Si=C}$ for the silenes **2**, **7**, and **8** (see Table 2) are, however, 14−17 Hz larger than those in 2-siloxysilenes, and they are significantly larger than $^1J_{Si-C}$ between silicon and carbon in alkylsilanes ($^1J_{Si-C} = 50.8$ Hz in $Me_3SiH$[34d]).

From the comparison between the accumulated theoretical data in Tables 1 and 2 and the experimental data for the decomposition products of siletanes **1**, **5**, and **6** it becomes evident that obviously none of the NMR spectroscopically detected species are free silenes. The deviation $\Delta\delta$ of the experimentally determined $\delta(^{29}Si)$ values from the calculated chemical shifts ranges from 94.7 ppm for silene **2** to 124.9 ppm for **8** and the calculated $^1J_{SiH}$ values for **1** and **7** are 38 and 37 Hz larger than the experimental values. Furthermore, the $\delta(^{13}C)$ chemical shift for **2** is predicted to be much more deshielded than that found for the decomposition product of **1** ($\Delta\delta = 95.5$). These large discrepancies are not due to principal deficiencies in the applied theoretical methods but suggest that the observed species formed in the condensed phase clearly are not free silenes, although these compounds have been identified in the gas phase by mass spectroscopy.

**Silene Dimethyl Ether Complexes.** Because of the inherent polarity of the Si=C bond silenes are best described as weak Lewis acids. The dimethyl-$d_6$ ether used as a lock substance for the NMR spectroscopic measurements is able to coordinate via its oxygen atom to the electrophilic silicon of the Si=C bond. Similar donor−acceptor complexes between silene **10** and amines, ethers, and the fluoride ion have been synthesized and structurally characterized in the solid state.[36] The complexation of **10** with ethers or amines has a decisive influence on $\delta(^{29}Si)$ in the corresponding adducts. For example, the $^{29}Si$ resonance of the THF complex **10**·THF (**15**) is shifted markedly by 91.8 ppm to higher field compared to the free silene. Also, the structural consequences of complexation are intriguing: the SiO separation in **15** is relatively small (1.878 Å), and the Si=C bond is elongated by 0.045 Å, suggesting a strong contribution of ylidic resonance structures.[36]

**Table 3. Calculated Association Energies $A_e$ (kcal mol$^{-1}$) for Complexes 16−18 (at the MP4(SDTQ)/6-311G(d)//B3LYP/6-311+G(2df,p) Level)**

| compd | $A_e$[a] | $A_e(0)$[b] | $A_e(133)$[c] |
|---|---|---|---|
| **16** | 5.4 | 4.1 | 5.2 |
| **17** | 5.5 | 4.6 | 5.7 |
| **18** | 5.6 | 5.1 | 6.2 |

[a] Theoretical association energy. [b] Association energy at 0 K. [c] Association energy at 133 K.

According to calculations at the MP4/6-311G(d)//B3LYP/6-311+G(2df,p) level (see Theoretical Methods), weakly bonded complexes **16**−**18** of silenes **2**, **7**, and **8** with dimethyl ether are stable toward dissociation. Their association energies $A_e$ (133 K), given in Table 3, are relatively small (ca 5.5 kcal mol$^{-1}$ at 133 K for **16**−**18**) which is typical for closed-shell interactions.[37] Complexes **16**−**18** not only are exothermic compounds but also are exergonic at 133 K; i.e., $\Delta G$ of formation of **18** at 133 K is −3.51 kcal mol$^{-1}$.

However, the quality of computed structures of weak donor−acceptor complexes in the gas phase depends strongly on the applied methods and basis sets. For a reliable description electron correlation and sufficiently large basis sets are prerequisites. The prediction of the structure of those complexes in the condensed phase is an even more complicated task. Numerous experimental investigations have shown that the distance between the donor and the acceptor in the gas phase is always longer than that in the solid state.[38] In a theoretical study Jonas et al. have shown that the differences between solid-state structures and calculated gas phase geometries for weakly bonded complexes are even more evident than for strongly bonded donor−acceptor complexes.[38a] From this it is obvious that weakly bonded adducts between silenes and dimethyl ether will have



(33) Apeloig, Y.; Bendikov, M.; Yuzefovich, M.; Nakash, M.; Bravo-Zhivotovskii, D.; Bläser, D.; Boese, R. *J. Am. Chem. Soc.* **1996**, *118*, 12228.

(34) (a) Schumann, C.; Dreeskamp, H. *J. Magn. Reson.* **1970**, *3*, 204. (b) Brook, A. G.; Abdesaken, F.; Gutekunst, G.; Plavec, N. *Organometallics* **1982**, *104*, 1349. (c) At the SOS/DFPT/IGLOIII level, the geometry is fully optimized at B3LYP/6-31G(d) in $C_s$ symmetry: $d$(Si=C) = 1.768 Å. (d) Harris, R. K.; Kimber, B. J. *J. Magn. Reson.* **1975**, *17*, 174.

(35) (a) Perdew, J. P.; Wang, Y. *Phys. Rev. B* **1992**, *45*, 13244. (b) Perdew, J. P. *Phys. Rev. B* **1986**, *33*, 8800. (c) Perdew, Y. *Phys. Rev. B* **1986**, *34*, 7406. (d) Kutzelnigg, W.; Fleischer, U.; Schindler, M. *NMR-Principles and Progress*; Springer-Verlag: Heidelberg, Germany, 1990; Vol. 23, p 165.

(36) Wiberg, N.; Wagner, G.; Reber, R.; Riede, J.; Müller, G. *Organometallics* **1987**, *6*, 35.

(37) The basis set superposition error for **16** is calculated to be 1.7 kcal mol$^{-1}$ at the MP4/6-311+G(d,p)/B3LYP/6-311+G(2df,p) level.

(38) (a) Jonas, V.; Frenking, G.; Reetz, M. T. *J. Am. Chem. Soc.* **1994**, *116*, 8741 and references cited therein. (b) A prominent example is the complex between $F_3B$ and HCN, for which a BN bond length of 1.638 ± 0.002 Å was determined by a single-crystal X-ray structure analysis, while the BN distance in the gas phase is increased by more than 50% (BN = 2.473 ± 0.029 Å): Burns, W. A.; Leopold, K. R. *J. Am. Chem. Soc.* **1993**, *115*, 11622.

**Table 4. Calculated Bond Lengths and Chemical Shifts of Complex 16 at Several Level of Theory**

| method | SiO | Si=C | $\delta(^{29}Si)^a$ | $\delta(^{13}C)^a$ |
|---|---|---|---|---|
| B3LYP/6-311+G(2df,p) | 2.553 | 1.705 | 58.5 | 74.4 |
| B3LYP/6-311+G(d,p) | 2.532 | 1.710 | 57.3 | 74.7 |
| B3LYP/6-311+G(d) | 2.540 | 1.710 | 57.8 | 72.4 |
| MP2/6-311+G(d,p) | 2.271 | 1.715 | 40.6 | 52.1 |
| QCISD/6-311+G(d,p) | 2.496 | 1.714 | 56.8 | 72.4 |
| B3LYP/6-311+G(2df,p)$^b$ | 2.164 | 1.715 | 22.5 | 48.0 |

[a] Calculated using B3LYP/GIAO/6-311+G(2df,p). [b] Calculated using the SCIPCM model.[39]

structures in solution quite different from those calculated for the gas phase. Thus, for a reliable structure description of the complexes **16**−**18** in solution an appropriate model chemistry is required which takes into consideration solvent effects and uses correlated methods with extended basis sets. This problem was tackled by following two different approaches. (i) The self-consistent polarized continuum model (SCIPCM)[39] was used to include solvent effects at the B3LYP/6-311+G(2df,p) level of theory in the geometry optimization of **16**. (ii) For an estimation of the influence of higher correlation methods on the SiO separation in **16** the structure was optimized at several correlated levels of theory, such as the second-order Møller−Plesset pertubation theory (MP2) and quadratic CI methods including single and double excitations (QCISD).[40] These results are summarized in Table 4.

The hybrid density functional method B3LYP using the extended 6-311+G(2df,p) basis set predicts an equilibrium SiO distance in **16** in the gas phase of 2.553 Å. The geometry of the silene subunit remains nearly unpertubed, as the Si=C bond length is only 0.002 Å longer than calculated for isolated **2** and the silicon center still has an almost trigonal-planar environment, as indicated by the sum of the bond angles Σ°, which is 358.2°. Nearly identical structures are obtained for the B3LYP calculations using the smaller basis sets 6-311+G(d,p) and 6-311+G(d). Geometry optimizations of **16** at the MP2/6-311+G(d,p) and QCISD/6-311+G(d) levels reveal that these higher correlated methods predict SiO separations which are markedly (0.261 Å (MP2) and 0.144 Å (QCISD)) smaller than anticipated from B3LYP calculations (see Table 4).

SCIPCM calculations suggest that the SiO separation in dimethyl ether solution ($\epsilon$ = 10.4 at 133 K) is strongly reduced by 0.389 Å, and both the pyramidalization at silicon and the Si=C bond length are increased (Σ° = 353.5°; $r$(Si=C) = 1.715 Å).

NMR chemical shift calculations on the different theoretical structures of **16** indicate $\delta(^{29}Si)$ and $\delta(^{13}C)$ to be highly sensitive toward variations of the SiO distance: both $\delta(^{29}Si)$ and $\delta(^{13}C)$ decrease strongly with decreasing SiO distance. This is exemplified by the SCIPCM calculations, which suggest that in ethereal solution the silene's silicon and carbon atoms are more shielded by 36.0 and by 26.4 ppm, respectively, than calculated for their gas-phase equilibrium structure (see Table 4). Similarly, for the MP2/6-311+G(d,p) optimized geometry $\delta(^{29}Si)$ and $\delta(^{13}C)$ (40.6 and 52.1 ppm, respectively) are calculated to be markedly high-field-shifted compared to the isolated silene. However, even the calculated NMR chemical shift data obtained from the SCIPM and from the MP2 or QCISD calculations deviate strongly from the experimental data obtained for **16**.

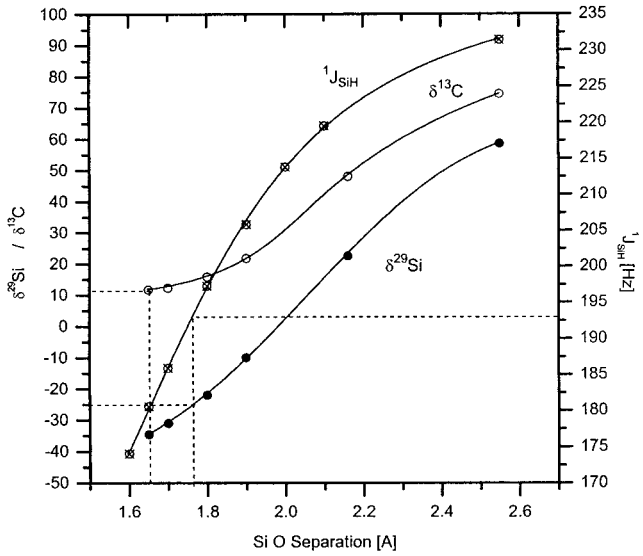


**Figure 8.** Calculated $\delta(^{29}Si)$, $\delta(^{13}C)$, and $^1J_{SiH}$ values of **16** as a function of the SiO separation ($\delta$ at the GIAO/B3LYP/6-311+G(2df,p)//B3LYP/6-311+G(2df,p) level and $^1J_{SiH}$ using SOS-DFPT/PP/IGLO/Basis III). The dotted lines indicate the experimental values for **16**.

These results suggest that in solution the true SiO distance in **16** is shorter than that predicted by the SCIPCM calculation and shorter than those found in the MP2 and QCISD computations. A combination of both, i.e., a SCIPCM calculation at a correlated (i.e., at MP2) level, would be required to describe correctly the structure of a complex such as **16**. However, such calculations are technically not feasible. Therefore, a potential energy scan for **16** along the SiO coordinate was performed at the B3LYP/6-311+G(2df,p) level. At several points along this scan the NMR chemical shift parameters and $^1J_{SiH}$ coupling constants were calculated using the B3LYP/GIAO/6-311+G(2df,p)[29] and the SOS-DFPT/IGLO/BIII methods,[30] respectively. In Figure 8 the theoretical $\delta(^{29}Si)$, $\delta(^{13}C)$, and $^1J_{SiH}$ values are plotted against different SiO distances and compared with the experimental results for **16**. This three-parameter fit of the theoretical data to the experimentally determined NMR parameters suggest an SiO distance for **16** of ca. 1.70−1.80 Å. [41]

Similarly, in Figure 9 the dependence of the computed chemical shifts on the SiO separations in the complexes **17** and **18** is shown. In accordance with Figure 8 a comparison between theoretically obtained values for $\delta(^{29}Si)$ with those detected experimentally leads for **17** and **18** to SiO distances of approximately 1.7 Å. Because

(39) Foresman, J. B.; Keith, T. A.; Wiberg, K. B.; Snoonian, J.; Frisch, M. J. *J. Phys. Chem.* **1996**, *100*, 16098.

(40) For an introduction to the applied methods and basis sets, see: (a) Hehre, W. J.; Radom, L.; Schleyer, P. v. R.; Pople, J. A. *Ab Initio Molecular Orbital Theory*; Wiley: New York, 1986. (b) Foresman, J. B.; Frisch, Æ. *Exploring Chemistry with Electronic Structure Methods*, 2nd ed.; Gaussian Inc.: Pittsburgh, PA, 1996.

(41) Taking into consideration that the GIAO/B3LYP/6-311+G(2df,p) method predicts both $\delta(^{29}Si)$ and $\delta(^{13}C)$ to be too deshielded compared to more sophisticated methods (compare Table 1, entries 1 and 2), leading to interceptions with the experimental values at overly small SiO separations, an actual SiO distance with a value between 1.7 and 1.8 Å is favored.

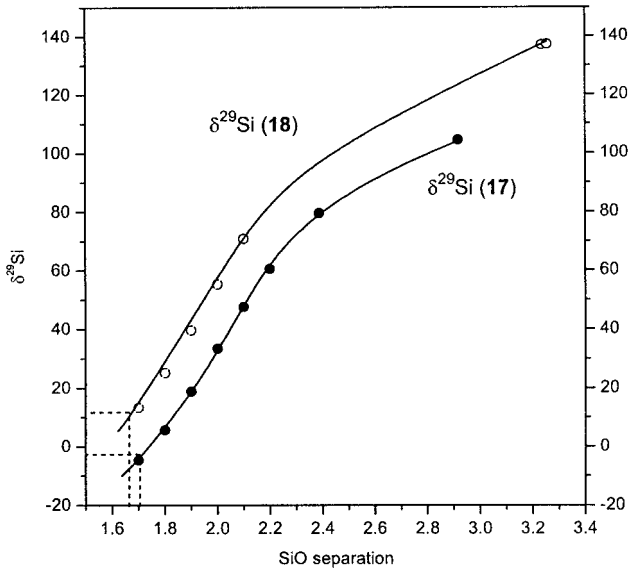


**Figure 9.** Calculated $\delta(^{29}Si)$ values of **17** and **18** as a function of the SiO separation (at the GIAO/B3LYP/6-311+G(2df,p)//B3LYP/6-311+G(2df,p) level). The dashed lines indicate the experimental $\delta(^{29}Si)$ values for **17** and **18**.

of the uncertainty of the theoretical determination of the NMR parameter a more accurate determination of the SiO distance is clearly not justified. It is, however, encouraging that the X-ray structure analysis of complex **15** between THF and the highly substituted silene **10** reveals a similarly short SiO distance of 1.878 Å.[36]

The electronic structure of donor−acceptor complexes has been the topic of many theoretical studies.[38] In a careful analysis Jonas et al. recently have shown that the donor−acceptor bond may predominantly be caused by either electrostatic or covalent interactions, the latter being induced by charge transfer from the donor to the acceptor.[38]

To obtain a deeper insight into the nature of the silene/ether donor−acceptor interactions, the results of the NBO population[42] scheme of complex **16** at different SiO distances are compared. The NBO analysis for the gas-phase equilibrium structure of **16** (see Table S1 of the Supporting Information) indicates only a small degree of charge transfer from $Me_2O$ to the silene. The occupation of the silene's acceptor $\pi^*$ orbital is only insignificantly increased by 0.02 e compared to its value in the isolated parent silene **2**. Accordingly, the charge transfer, as computed by the summation over all atomic charges of the silene and of the dimethyl ether, is merely 0.04e. Consequently, the total SiO bond order as predicted by the natural resonance theory is very small (0.02) and the donor−acceptor interaction is completely ionic in its nature. The charge transfer between silene and ether increases with decreasing SiO distance. This is convincingly shown by the growing occupation of the $\pi^*$ acceptor orbital of the silene (0.14e at a SiO distance of 1.7 Å) and the depletion of the lone pairs on oxygen (1.82e, 1.96e) compared to free dimethyl ether (1.94e, 1.97e). For a SiO separation of 1.7 Å the charge transfer

**Scheme 6**

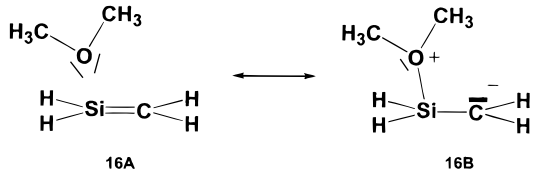

16A 16B

reaches 0.15 e but the SiO bond order is still very small (0.09) and nearly exclusively ionic. In the silene−ether complex **16** the Si=C bond is more polarized than in silene **2** and the ionic contribution becomes even larger with decreasing SiO distance. Thus, while in silene **2** the ionic contribution to the bond order is one-third of the total value, it is approximately 50% in **16** at SiO distances shorter than 1.9 Å. This clearly indicates the importance of the ionic resonance structure **16B** to describe the nature of the Si=C bond in the donor silene complex **16** (Scheme 6).

## Conclusion

The parent silene **2**, 1-methylsilene (**7**), and 1,1-dimethylsilene (**8**) have been prepared by low-pressure flow pyrolysis from the corresponding siletanes **1**, **5**, and **6**. The highly reactive silenes can be condensed and stored at liquid-nitrogen temperatures for days without decomposition. **2**, **7,** and **8** were identified by residual gas analysis of the pyrolysis stream and by low-temperature NMR spectroscopy of their complexes **16**−**18** with dimethyl ether. Solutions of the silenes in dimethyl ether and $CCl_2F_2$ are stable up to temperatures between −140 and −100 °C. Above these temperatures rapid polymerization occurs. In particular, under the applied conditions, the dimerization products, 1,3-disiletanes, the usual subsequent products of reactive alkylsilenes, are not formed. The complexation with dimethyl ether obviously stabilizes the silenes and allows their spectroscopic investigation. These experimental results are supported by ab initio and density functional calculations of geometries and magnetic properties of the silenes **2**, **7**, and **8** and the donor−acceptor complexes **16**−**18**. The calculations suggest a relatively short Si−O separation of about 1.7−1.8 Å in the corresponding silene−ether adducts. Natural bond analysis of the wave function of the donor−acceptor complex **16** reveals that the interaction between the ether molecule and the silene is predominantly ionic despite the relatively short SiO distance.

## Theoretical Methods

The geometries of the silenes **2**, **7**, and **8** and their complexes with dimethyl ether **16**−**18** have been uniformely optimized[43] employing Becke's three-parameter hybrid method using the

(42) (a) Glendening, E. D.; Badenhoop, J. K.; Reed, A. E.; Carpenter, J. E.; Weinhold, F. NBO 4.0; Theoretical Chemistry Institute, University of Wisconsin, Madison, WI, 1996. (b) Reed, A. E.; Curtiss, L. A.; Weinhold, F. *Chem. Rev.* **1988**, *88*, 899.

(43) All calculations were performed with Gaussian 94: Frisch, M. J.; Trucks, G. W.; Schlegel, H. B.; Gill, P. M. W.; Johnson, B. G.; Robb, M. A.; Cheeseman, J. R.; Keith, T.; Petersson, G. A.; Montgomery, J. A.; Raghavachari, K.; Al-Laham, M. A.; Zakrzewski, V. G.; Ortiz, J. V.; Foresman, J. B.; Cioslowski, J.; Stefanov, B. B.; Nanayakkara, A.; Challacombe, M.; Peng, C. Y.; Ayala, P. Y.; Chen, W.; Wong, M. W.; Andres, J. L.; Replogle, E. S.; Gomperts, R.; Martin, R. L.; Fox, D. J.; Binkley, J. S.; Defrees, J. S.; Baker, J.; Stewart, J. P.; Head-Gordon, M.; Gonzalez, C.; Pople, J. A. Gaussian 94, Revisions C.2-E2; Gaussian, Inc., Pittsburgh, PA, 1995.

LYP correlational functional (B3LYP)[44] and the 6-311+G(2df,p) basis set. Frequency calculations at this level have been performed to verify minimum structures.[40] Theoretical association energies $A_e$ between silenes **2**, **7**, and **8** and dimethyl ether have been calculated using MP4(SDTQ) single-point energies utilizing the 6-311G(d) basis set. Those energies have been refined by adding zero-point energies calculated at B3LYP/6-311+G(2df,p), giving the association energy in the gas phase at 0 K ($A_e(0)$). Association energies at 133 K ($A_e(133)$) have been estimated by using an empirical correction of $^1/_2RT$ per rotational or translational degree of freedom and $RT$ for the work term $pV$. The SiO separation in **16**−**18** is very sensitive to the applied method and basis set (see above). The influence of higher correlation methods on the SiO distance has been tested for **16**, which was also optimized at the MP2 and QCISD level employing the somewhat smaller 6-311+G(d,p) and 6-311+G(d) basis sets. Solvent effects have been modeled at the B3LYP/6-311+G(2df,p) level of theory using the self-consistent polarized continuum model (SCIPCM,[39] dielectricity constant $\epsilon = 10.4$, isodensity value 0.0004 au). Potential energy scans along the SiO coordinate of the potential energy surface have been calculated at the B3LYP/6-311+G(2df,p)//B3LYP/6-311+G(2df,p) level of theory.

NMR chemical shift calculations have been uniformly performed using the GIAO method at the B3LYP/6-311+G(2df,p) level,[29] and the performance of this approach has been compared for **2** using GIAO/MP2/tz2p(Si,C)dzp(H) calculations.[31] Spin−spin coupling constants have been calculated using the SOS/DFPT/IGLO approach[30] developed by Malkin and Malkina as implemented in deMon NMR code.[45] For the calculation of the spin−spin coupling constants the Perdew exchange functional,[35a,b] the extra fine grid option with 64 points of radial quadrature,[30b,45] and the basis set III[35c] have been used. The electronic structure of complex **16** was analyzed using NBO theory.[42]

## Experimental Section

Siletanes **1**, **5**, and **6** were synthesized from (3-chloropropyl)-chlorosilanes by reductive cyclization according to literature procedures.[14,46]

Dimethyl-$d_6$ ether was prepared by dehydration of methanol-$d_4$.[47] For the residual gas analysis a quadrupole mass spectrometer EQ50 (Edwards, IP 90 eV, *m*/*e*(max) 200) was used. $^1$H, $^{13}$C, and $^{29}$Si NMR spectra of the solutions of the pyrolysis products were measured on a Bruker WM300 NMR spectrometer using a broad-band probe. TMS was used as external standard. The probe temperature was calibrated with a $^{13}$C chemical shift thermometer using neat 2-chlorobutane[48] in a capillary in an NMR tube filled with $(CD_3)_2O/CF_2Cl_2$.

**Low-Pressure Pyrolysis of Siletanes 1, 5, and 6.** The complete pyrolysis apparatus[14] was evacuated to a final pressure of $10^{-9}$ mbar and was heated to 250 °C for 24 h. The chemical composition of the pyrolysis gas stream was analyzed by a quadrupole mass spectrometer, and the optimal pyrolysis conditions with respect to pyrolysis temperature and pressure for each siletane had been determined in previous runs. For the preparation of NMR samples, 10 mmol of the siletane was pyrolyzed over a period of 6 days at oven temperatures of 900−1000 °C. The pressure in the pyrolysis tube rises typically to $10^{-4}$−$10^{-5}$ mbar. The pyrolysis products were collected and condensed in the cooling trap at −196 °C, and the produced ethene was pumped off. The molten glasslike, highly viscous condensate was then transferred into an adjoining 10 mm NMR tube. As both lock compound and solvent for the NMR measurements, 2.5 mL of dimethyl-$d_6$ ether and dichlorodifluoromethane in an approximately 1:4 ratio were condensed into the NMR tube after the pyrolysis was completed. This mixture remains liquid even at about −140 °C, the temperature required for the NMR measurements. Residual ethene was pumped off at −196 °C, and then the NMR tube was sealed under ultrahigh vacuum (approximately $10^{-9}$ mbar) and was stored in liquid nitrogen until the NMR investigations were performed.

**16**: $^1$H NMR (300 MHz, $CF_2Cl_2/(D_3C)_2O$, −140 °C) $\delta$ 5.80−6.90; $^{13}$C NMR (75.5 MHz, $CF_2Cl_2/(D_3C)_2O$, −140 °C) $\delta$ 10.8 ($^1J_{CH}$ = 137 Hz); $^{29}$Si NMR (59.6 MHz, $CF_2Cl_2/(D_3C)_2O$, −140 °C) $\delta$ −25.2 ($^1J_{SiH}$ = 193 Hz).

**17**: $^{29}$Si NMR (59.6 MHz, $CF_2Cl_2/(D_3C)_2O$, −140 °C) $\delta$ −1.8 ($^1J_{SiH}$ = 180 Hz).

**18**: $^{29}$Si NMR (59.6 MHz, $CF_2Cl_2/(D_3C)_2O$, −135 °C) $\delta$ 16.8.

**Acknowledgment.** This work was supported by the DFG and by the German Israeli Foundation (GIF). T.M. thanks the Fonds der Chemischen Industrie and the DFG for scholarships. We are indebted to the computer center of the Humboldt University Berlin for large amounts of computer time and for excellent services.

**Supporting Information Available:** Detailed description and figure of the pyrolysis apparatus and a table with NBO results. This material is available free of charge via the Internet at http://pubs.acs.org.

OM0002778

(44) (a) Becke, A. D. *Phys. Rev.* **1988**, *A 38*, 3098. (b) Becke, A. D. *J. Chem. Phys.* **1993**, *98*, 5648. (c) Johnson, B. G.; Gill, P. M. W.; Pople, J. A. *J. Chem. Phys.* **1993**, *98*, 5612.

(45) de Mon program: (a) Salahub, D. R.; Fournier, R.; Mlynarski, P.; Papai, I.; St-Amant, A.; Ushio, J. In *Density Functional Methods in Chemistry*; Labanowski, J., Andzelm, J., Eds.; Springer: New York, 1991. (b) St-Amant, A.; Salahub, D. R. *Chem. Phys. Lett.* **1990**, *169*, 387.

(46) (a) Damrauer, R. *Chem. Rev. A* **1972**, *8*, 67. (b) Dubac, J.; Mazerolles, P.; Lesbre, M.; Joly, M. *J. Organomet. Chem.* **1977**, *99*, 2390. (c) Laane, J. *J. Am. Chem. Soc.* **1967**, *89*, 1144. (d) Auner, N.; Grobe, J. *J. Organomet. Chem.* **1980**, *188*, 25.

(47) Erlenmeyer, E.; Kriechbaumer, A. *Ber. Dtsch. Chem. Ges.* **1874**, *7*, 699.

(48) Schneider, H.-J.; Freitag, W. J. *J. Am. Chem. Soc.* **1976**, *98*, 978.